Epithelial-mesenchymal transition can suppress major attributes of epithelial tumor-initiating cells

Toni Celià-Terrassa, Óscar Meca-Cortés, Francesca Mateo, Alexia Martínez de Paz, Nuria Rubio, Anna Arnal-Estapé, Brian J. Ell, Raquel Bermudo, Alba Díaz, Marta Guerra-Rebollo, Juan José Lozano, Conchi Estarás, Catalina Ulloa, Daniel Álvarez-Simón, Jordi Milà, Ramón Vilella, Rosanna Paciucci, Marian Martínez-Balbás, Antonio García de Herreros, Roger R. Gomis, Yibin Kang, Jerónimo Blanco, Pedro L. Fernández, and Timothy M. Thomson

Contents:

Supplemental Methods

Sources of primary antibodies to: E-cadherin intracytoplasmic domain (clone 36); E-cadherin extracellular domain (clone HECD-1), EpCAM (B29.1/VU-ID9), trimethyl histone H3K4 (Abcam, Cambridge, UK); fibronectin, ZEB1 (Sigma); vimentin (clone V9, Labvision); SOX2 (clone D6D9, Cell Signaling); human SNAI1 (SN9H2), human TWIST1 (Cell Signaling); actin (I-19), CD44 (DF1485, or produced and purified in-house from hybridoma 33-3B3), SPARC (H-90), CD24 (ML5), CD40 (LOB-11), luciferase (251-550) (Santa Cruz Biotechnology, Santa Cruz, CA); CD71 (produced and purified in-house from hybridoma 120-2A3); acetyl histone H3, acetyl histone H4, trimethyl histone H3K27 (Upstate Millipore, Billerica, MA); hemagglutinin (Clone 3F10, Roche, Diagnostics, Mannheim, Germany); MYC (Epitomics, Burlingame, CA). LiCl and MG132 were from Sigma.

Growth curves. Cells (5 x 10^3/well) were seeded in sextuplicate in 96-well plates (Costar, Corning, NY). All cells used have the firefly luciferase gene stably integrated in their genomes. Standard curves were generated to correlate cell numbers to luminescence levels yielded by cell lysates, using the Luciferase Reporter Assay Kit (Promega, Madison, WI). For growth curves, cells were harvested daily for 6 or 7 consecutive days, luminescence quantified, and cell numbers extrapolated on the basis of standard curves. Luminescence was quantified either on a Victor 3 instrument (Perkin-Elmer, Wellesley, MA) or an OrionII Microplate Luminometer (Berthold Detection Systems, Pforzheim, Germany).

Wound healing assays. Cells (2 x 10^5/well) were seeded in 24-well plates, allowed to reach confluent monolayers and serum-starved for 24 h. Wounds were created with a 0.5 mm plastic pipette tip. Afterwards, cells were fed with medium with 0.5% or 10% FBS, to create differential healing conditions. Images were captured and surface areas between leading edges of the monolayers at predetermined wound sites (3 sites per condition, performed in triplicate) were measured for the following 54 h and analyzed with the ImageJ software.

Cell cycle analysis. Cells were seeded in 6-well plates (Costar), detached with Trypsin/EDTA/1% BSA, washed twice and resuspended in PBS, followed by dropwise addition of 70% ethanol and fixation at 4 ºC for 2 h. Subsequently, fixed cells were

washed twice with PBS/50 mM EDTA/1% BSA, incubated with 1 mg/mL RNase A (Sigma) at 37ºC for 1 h, and 0.1 mg/mL propidium iodide (Sigma). DNA content was determined with a Cytomics FC500 instrument (Coulter, Hialeah, FL), and cell cycle distribution analyzed with the Multicycle program coupled to the instrument. All cell cycle determinations were done in triplicate.

***In vivo* tumorigenic assays**. For orthotopic implantation, 10^5 cells in a volume of 25 μL were inoculated in the ventral lobe of anesthetized 6-week-old male NOD-SCID mice. Eight mice were implanted for each cell type analyzed. To assess localized growth, cells were xenografted by intramuscular injection in 6-week-old male NOD-SCID mice, 4 mice for each cell line. The injections were 2.5 x 10^5 cells in a volume of 50 μL RPMI 1640 (without FBS) in each hind limb (2 injection sites per mouse). Tumor growth was monitored once or twice a week by luminometry on an ORCA-2BT instrument (Hamamatsu Photonics, Hamamatsu, Japan). Images and light counts were initiated 5 min after intraperitoneal injection of luciferine (100 mg/Kg in 150 μL). Animals were allowed to form tumors up to 1.5 cm in diameter, at which point they were euthanized. To monitor metastatic growth after orthotopic implantation experiments, separate images and photon counts were obtained for the thoracic (anterior) and abdominal (posterior) areas of mice. The images obtained were analyzed by the Hokawo 2.1 software (Hamamatsu Photonics). To assess lung colony formation, 2.5 x 10^5 cells in 150 μL RPMI 1640 (without FBS) were injected through the dorsal caudal vein of anesthetized 6-week-old male NOD-SCID mice (6 mice per cell line). The images obtained were analyzed with the Hokawo 2.1 software. To assess colonization to other organs, 2 x 10^5 cells in 100 μL PBS were injected in the left ventricle of anesthetized 6-week-old Balb c/nude, NOD-SCID or athymic Ncr-nu/nu mice (6 to 10 mice per cell line). Mice were imaged immediately after injection and thereafter tumor development was monitored by weekly imaging on an IVIS-200 instrument (Xenogen-Caliper Life Sciences, Hopkinton, MA) after retroorbital injection of 1.5 mg luciferine (15 mg/mL in PBS). For bioluminescence plots, photon flux was calculated for each mouse by using a circular region of interest of the mouse in a supine position. This value was scaled to a comparable background value (from a luciferin-injected mouse with no tumor cells), and then normalized to the value obtained immediately after xenografting at the same area (day 0), so that all mice had an arbitrary starting Bioluminiscent I signal of 10,000. Lesions were localized by *ex vivo* bioluminescence imaging and resected under sterile

conditions. Some of the lesions were fixed with formalin and processed for histological analysis. Statistics: in lung colonization and bone metastasis free survival analysis, lesions that had an increased photon flux value above day 0 were counted as events. Statistics were performed by Log Rank (Mantel-Cox) test using SPSS software. For PC-3/S-CDH1 and PC-3/S-SOX2 tumor growth, cells (2×10^5) were implanted i.m. into 6-week old male Swiss-nude mice and tumor size monitored with a caliper. For serial xenotransplantation experiments, 10^3, 10^4 or 10^5 cells were implanted i.m. in the hind limbs of anesthetized 6-week-old male Swiss-Nude mice. Tumors formed by implantation of 10^5 cells were extracted, subjected to mechanical disgregation and digestion with 300 U/mL collagenase A (Sigma) in Hank's Balanced Salt Solution (PAA) for 30 min at 37ºC, selected for neomycin resistance for 7 d in order to remove contaminating mouse cells, and reimplanted i.m. in a second series of animals, as above. This process was repeated in a third series of animals. Tumor growth was monitored with a caliper, and tumor volumes calculated as described in (1).

RNA isolation, reverse transcription and transcriptomic analysis. Cells were grown to 70-80% confluence, lysed and RNA isolated with the RNeasy Kit (Qiagen, Hilden, Germany), including a DNase digestion step. For microarray analysis, RNAs were amplified, labeled and hybridized to Affymetrix U133 2.0 Plus arrays (Affymetrix, Santa Clara, CA). Microarray data were normalized using the robust multi-array (RMA) algorithm (2). Next, we employed a conservative probe-filtering step, eliminating those probes with a maximum expression value lower than 5. To identify differentially expressed genes, we applied Significance Analysis of Microarrays (SAM-R) (3), selecting those genes with a False Discovery Rate (FDR) below 10% ($Q < 10$). Comparative transcriptomic analysis was performed on independent triplicate samples.

Gene set enrichment analysis. For comparative pathway and gene set correlations, Gene Set Enrichment Analysis (GSEA) (4, 5) was applied in order to identify overrepresented predefined gene sets using C2 and C5 genesets from MSigDB v3. Additionally, 4 reported gene sets (ESC-like module (6), MYC module (7), ES1 and ES2 modules (10)) were analyzed for their representation in PC-3/Mc and PC-3/S cells using normalized microarray expression data. Gene-set permutation type with 1,000 random permutations was run to obtain a rank gene list, enrichment plots and heat maps. For GSEA of a previously published prostate cancer expression dataset (11), a gene set was generated consisting of a subset of genes of the ESC-like module most

significantly enriched in PC-3/Mc cells (M geneset) and used to run GSEA on a continuous phenotype modality, in which a numerical variable was generated for three values corresponding to metastatic samples (class 1), primary tumor samples with pathological stages T3 or T4 (class 2) and primary tumor samples with pathological stages T1 or T2 (class 3), and a Pearson correlation was applied as the metric to determine correlations the representation of the M geneset and these three classes of samples taken as continuous variables (http://www.broadinstitute.org/gsea/doc/GSEAUserGuideFrame.html?_Metrics_for_Ranking).

Real-time RT-PCR (qPCR). Complementary DNAs were synthesized with the High-Capacity cDNA Reverse Transcription Kit (Applied Biosystems, Carlsbad, CA). Real-time quantitative PCR assays were performed in a LightCycler 480 instrument (Roche Diagnostics) and analyzed with the LightCycler 480 Software release 1.5.0. Either gene-specific TaqMan assays (Applied Biosystems) or the Universal Probe Library system (UPL; Roche) were used, following the specific running conditions recommended in each case. The following transcripts were quantified with TaqMan assays (Supplemental Table 10): *SOX2*, *RUNX2* and *TWIST2*. The following transcripts were quantified with the UPL system (Supplemental Table 11): *NANOG*, *LIN28A*, *KLF9*, *KLF4*, *MYC*, *POU5F1* (*OCT4*), *SNAI1*, *SNAI2*, *ZEB1*, *ZEB2*, *TWIST1*, *RUNX1*, *CDH1*, *DSP*, *TACSTD1*, *CDH2*, *SPARC*, *VIM* and *FN1*. The amplification levels of *RN18S1* and HMBS were used as an internal reference to estimate the relative levels of specific transcripts, and relative quantification was determined by the ΔΔCp method. All determinations were done in triplicate and values represented as $\log_{10}$ of $2^{-\Delta\Delta Cp}$ (12). In some cases in which transcriptional profiles from multiple samples were compared, relative expression values were represented as a heatmap with pseudocoloring ranging from green (underexpressed relative to values in control cells) to red (overexpressed relative to control cells).

Cell surface immunophenotyping. Cells were detached with PBS/2 mM EDTA for 20-30 min, washed, incubated with primary antibody diluted 1:20 in PBS/3% normal goat serum for 30 min in a shaker at 4 °C, washed, incubated with the secondary antibody (Alexa Fluor 488, anti-mouse, 1:200 dilution; Invitrogen) for 30 min, washed and analyzed by flow cytometry on a Cytomics FC500 instrument (Coulter, Hialeah, FL)

Immunocytochemistry. Sterile coverslips placed at the bottom of 24-well plates were seeded with 3 x 10^4 cells, allowed to attach for 72 h, washed with PBS and fixed for 1 h with methanol at -20 ºC. After fixation, samples were washed with acetone, then 5 times with PBS, blocked for 30 min with blocking buffer (5% normal goat serum, 0.5% Triton X-100 in PBS) and incubated with anti-E-cadherin (1:100; Clone 36; Becton-Dickinson), anti-SNAI1 (1:20) or anti-SOX2 (1:50) for 2 h at room temperature. This was followed by PBS washes, a 1 h incubation with Alexa Fluor 488-conjugated goat-anti-mouse IgG (1:1,000), and final washes followed by incubation with DAPI (1:1,000; Sigma) for 10 min. Coverslips were mounted on slides with Mowiol 4-88 and images captured with a Leica SP5 confocal microscope.

Immunoblotting. Cell lysates were boiled in Laemmli sample buffer, electrophoresed by SDS-PAGE, transferred to PVDF membranes (Immobilon-FL; Millipore, Billerica, MA) and blotted with antibodies to human E-cadherin (1:8,000), vimentin (1:2,000), fibronectin (1:500), SNAI1 (1:500), TWIST1 (1:1,000), SOX2 (1:1,000), MYC (1:1,000), SPARC (1:500), EpCAM (1:500), ZEB1 (1:1,000), actin (1:2,000). Reactions were detected with fluorescent dye-conjugated secondary antibodies (IRDye 800CW Goat Anti-Mouse IgG; IRDye 680 Goat Anti-Rabbit IgG; IRDye 680 Donkey Anti-Goat IgG) on an Odyssey infrared imaging system (Li-COR Biosciences, Lincoln, NE). Sample loadings were normalized by detection of actin or β-tubulin levels.

Chromatin immunoprecipitation (ChIP). The procedure followed that described by Kimura *et al*. (13). Briefly, 7 x 10^5 cells were collected and fixed with 1% formaldehyde in PBS, centrifuged and washed twice with PBS. Then, cells were resuspended in 300 µL lysis buffer (10% SDS, 10 mM EDTA, 1 M Tris pH 8, 100 mM PMSF, 1µg/µL leupeptin, 1µg/µL aprotinin, 1 M Na_5VO_4). Cell lysates were sonicated in a BioRuptor sonicator at maximum potency for 13 min. Chromatin was pre-cleared with 5% salmon sperm DNA (2 µg) / Protein A Agarose (Millipore) for 2 h at 4 ºC. Immunoprecipitation was performed by incubation with 2 µg of primary antibodies in 5% salmon sperm DNA (2 µg) /Protein A agarose overnight at 4ºC. As a negative control, 2 µg of normal rabbit IgG was used. Specific DNA segments from the immunoprecipitated material were amplified with primers for selected gene promoters, and the PCR products were quantified by SYBRGreen incorporation under real-time conditions in a LightCycler 480 Instrument (Roche). The primers used for amplification (sequences as shown

below) were designed within the 1 Kb region upstream of the transcript start site for each gene, with the help of the LightCycler Probe Design2 Software (Roche), and were tested for specificity and efficiency of amplification prior to their use in ChIP (Supplemental Table 12). The results are expressed as specific amplification levels on immunoprecipitated DNA relative to the amplification levels yielded by input DNA. All determinations were done in triplicate.

Production and transduction of retroviral particles. Construct pBABEpuro-Twist1 (mouse) was kindly provided by Dr. Gabriel Gil (IMIM, Barcelona). pBABEpuro-Snai1-HA (mouse), pMSCV-Flag-SOX2 (human) and pWZL-Blast-E-cadherin (mouse) have been described (14-16). pBABEpuro-HA-TWIST2 was constructed inserting full-length human TWIST2 cDNA into pCMV-HA in frame with the hemagglutinin epitope and then into pBABEpuro. The retrovirus packaging cell line PG13 was co-transfected with these DNAs and pVSV-G (Clontech, Mountain View, CA) for 12 h using Fugene HD (Roche). Supernatants were collected during the following 48 h and filtered through 0.45 μm methylcellulose filters (Millipore). Retroviral particles were concentrated by ultracentrifugation at 27,000 rpm for 90 minutes on 20% sucrose density gradients. Viral particles were resupended with medium and added to the cells together with 8 μg/mL polybrene (Sigma). Plates were centrifuged at 1,800 rpm for 60 minutes and cells allowed to recover in fresh medium for 24-48 h. Cells with integrated retroviral sequences were selected for 5 days in medium supplemented with 3 μg/mL puromycin (Biomol) for PC-3/Mc cells or 1 μg/mL puromycin for TSU-Pr1-B2 cells. PC-3/S cells transduced with pWZL-Blast-E-cadherin were selected with 25 μg/mL blastocydin for 10 d.

Production and transduction of lentiviral particles. Constructs pLKOpuro-shRNA-CDH1 (TRCN0000039665 and TRCN0000039666), pLKOpuro-shRNA-SOX2 (TRCN0000003252, TRCN0000003253 and TRCN0000010772), pLKOpuro-shRNA-KLF4 (TRCN0000005314, TRCN0000005313, TRCN0000005315 and TRCN0000005316), pLKOpuro-shRNA-MYC (TRCN0000039640, TRCN0000039641 and TRCN0000039642), pLKOpuro-shRNA-SNAI1 (TRCN0000063819, TRCN0000063818, TRCN0000063820, TRCN0000063821 and TRCN0000063822), pLKOpuro-shRNA-TWIST2 (TRCN0000020869, TRCN0000020870, TRCN0000020871 and TRCN0000020872) and pLKOpuro-shRNA-ZEB1

(TRCN0000017565, TRCN0000017563, TRCN0000017564 and TRCN0000017566) and the non-target control vector Shc002 were purchased from Sigma-Aldrich. The bicistronic expression vectors pRRL-Luc-IRES-EGFP and pRRL-Renilla-IRES-RFP were as described (17). The lentivirus packaging cell line HEK293T was co-transfected with these DNAs, pCMVdeltaR8.91 and pVSV-G (Clontech, Mountain View, CA) for 12 h using Fugene HD (Roche). Supernatants were collected for the following 48 h and filtered through 0.45 μm methylcellulose filters (Millipore). Lentiviral particles were concentrated by ultracentrifugation at 27,000 rpm for 90 minutes on 20% sucrose density gradients. Viral particles were resupended with medium and added to the cells together with 8 μg/mL polybrene (Sigma). Cells were infected for 24 hours and allowed to recover in fresh medium for 24-48 h. Selection for cells with integrated lentiviral sequences was performed as above.

Immunohistochemistry. Two μm thick sections were obtained for immunohistochemistry either from formalin-fixed and paraffin-embedded tissue blocks or from tissue microarrays (TMA), built with a Manual Tissue Arrayer 1 (Beecher Instruments, Sun Prairie, WI). A total of 99 tumors, 37 normal samples from human specimens were analyzed, as well as tumors from immunodeficient mouse xenografts. Tissue sections were mounted on xylaned glass slides (DAKO, Glostrup, Denmark) and used for immunohistochemical staining using the Bond Polymer Refine Detection System (Leica, Wetzlar, Germany). Samples were deparaffinized, antigen retrieval performed at pH 6 for 20 minutes and primary antibodies incubated for 1 hour. Antibody dilutions used were 1:50 for SOX2 (Clone D6D9, Cell Signaling) and 1:50 or 1:150 for E-cadherin (NCL-E, Novocastra, Newcastle, UK) on mouse and human samples, respectively. SOX2 staining was scored as the percentage of cells with nuclear positivity and the predominant staining intensity. E-cadherin staining was assessed as a percentage of membrane or cytoplasmic pattern. Images were captured with an Olympus BX-51 microscope equipped with an Olympus DP70 camera. Human tissues were procured from patients at the Hospital Clínic of Barcelona after informed consent by the patients and approval by the Institutional Ethics Committee.

Immunofluorescence of tumors from xenograft experiments. Tumors from xenografted mice were snap-frozen in OCT and 2-μm sections fixed in 4% paraformaldehyde for 15 min, washed twice with PBS and incubated with blocking

solution (0.2% saponin, 5% normal goat serum in PBS). Primary antibodies were incubated for 2 h, washed with PBS, incubated with fluorescent-conjugated secondary antibodies, washed and counterstained with DAPI (1:1,000; Sigma). Slides were mounted with Mowiol 4-88 and images captured with a Leica SP5 confocal microscope. Rabbit anti-luciferase (Santa Cruz) was used at 1:100. As a secondary antibody, Alexa Fluor 647-conjugated goat-anti-rabbit IgG (Invitrogen) was used at 1:200.

Supplemental References

1. Feldman, J.P., Goldwasser, R., Mark, S., Schwartz, J., and Orion, I. 2009. A mathematical model for tumor volume evaluation using two-dimensions. *J Appl Quant Meth* 4:455-462.
2. Irizarry, R.A., Bolstad, B.M., Collin, F., Cope, L.M., Hobbs, B., and Speed, T.P. 2003. Summaries of Affymetrix GeneChip probe level data. *Nucleic Acids Res* 31:e15.
3. Tusher, V.G., Tibshirani, R., and Chu, G. 2001. Significance analysis of microarrays applied to the ionizing radiation response. *Proc Natl Acad Sci U S A* 98:5116-5121.
4. Mootha, V.K., Lindgren, C.M., Eriksson, K.F., Subramanian, A., Sihag, S., Lehar, J., Puigserver, P., Carlsson, E., Ridderstrale, M., Laurila, E., et al. 2003. PGC-1alpha-responsive genes involved in oxidative phosphorylation are coordinately downregulated in human diabetes. *Nat Genet* 34:267-273.
5. Subramanian, A., Tamayo, P., Mootha, V.K., Mukherjee, S., Ebert, B.L., Gillette, M.A., Paulovich, A., Pomeroy, S.L., Golub, T.R., Lander, E.S., et al. 2005. Gene set enrichment analysis: a knowledge-based approach for interpreting genome-wide expression profiles. *Proc Natl Acad Sci U S A* 102:15545-15550.
6. Wong, D.J., Liu, H., Ridky, T.W., Cassarino, D., Segal, E., and Chang, H.Y. 2008. Module map of stem cell genes guides creation of epithelial cancer stem cells. *Cell Stem Cell* 2:333-344.
7. Kim, J., Woo, A.J., Chu, J., Snow, J.W., Fujiwara, Y., Kim, C.G., Cantor, A.B., and Orkin, S.H. 2010. A Myc network accounts for similarities between embryonic stem and cancer cell transcription programs. *Cell* 143:313-324.
8. Boyer, L.A., Lee, T.I., Cole, M.F., Johnstone, S.E., Levine, S.S., Zucker, J.P., Guenther, M.G., Kumar, R.M., Murray, H.L., Jenner, R.G., et al. 2005. Core transcriptional regulatory circuitry in human embryonic stem cells. *Cell* 122:947-956.
9. Wang, J., Rao, S., Chu, J., Shen, X., Levasseur, D.N., Theunissen, T.W., and Orkin, S.H. 2006. A protein interaction network for pluripotency of embryonic stem cells. *Nature* 444:364-368.
10. Ben-Porath, I., Thomson, M.W., Carey, V.J., Ge, R., Bell, G.W., Regev, A., and Weinberg, R.A. 2008. An embryonic stem cell-like gene expression signature in poorly differentiated aggressive human tumors. *Nat Genet* 40:499-507.
11. Taylor, B.S., Schultz, N., Hieronymus, H., Gopalan, A., Xiao, Y., Carver, B.S., Arora, V.K., Kaushik, P., Cerami, E., Reva, B., et al. 2010. Integrative genomic profiling of human prostate cancer. *Cancer Cell* 18:11-22.
12. http://www3.appliedbiosystems.com/cms/groups/mcb_support/documents/generaldocuments/cms_040980.pdf.
13. Kimura, H., Hayashi-Takanaka, Y., Goto, Y., Takizawa, N., and Nozaki, N. 2008. The organization of histone H3 modifications as revealed by a panel of specific monoclonal antibodies. *Cell Struct Funct* 33:61-73.
14. Aasen, T., Raya, A., Barrero, M.J., Garreta, E., Consiglio, A., Gonzalez, F., Vassena, R., Bilic, J., Pekarik, V., Tiscornia, G., et al. 2008. Efficient and rapid generation of induced pluripotent stem cells from human keratinocytes. *Nat Biotechnol* 26:1276-1284.

15. Batlle, E., Sancho, E., Franci, C., Dominguez, D., Monfar, M., Baulida, J., and Garcia De Herreros, A. 2000. The transcription factor snail is a repressor of E-cadherin gene expression in epithelial tumor cells. *Nat Cell Biol* 2:84-89.
16. Onder, T.T., Gupta, P.B., Mani, S.A., Yang, J., Lander, E.S., and Weinberg, R.A. 2008. Loss of E-cadherin promotes metastasis via multiple downstream transcriptional pathways. *Cancer Res* 68:3645-3654.
17. Degano, I.R., Vilalta, M., Bago, J.R., Matthies, A.M., Hubbell, J.A., Dimitriou, H., Bianco, P., Rubio, N., and Blanco, J. 2008. Bioluminescence imaging of calvarial bone repair using bone marrow and adipose tissue-derived mesenchymal stem cells. *Biomaterials* 29:427-437.
18. Peiro, S., Escriva, M., Puig, I., Barbera, M.J., Dave, N., Herranz, N., Larriba, M.J., Takkunen, M., Franci, C., Munoz, A., et al. 2006. Snail1 transcriptional repressor binds to its own promoter and controls its expression. *Nucleic Acids Res* 34:2077-2084.

Supplemental Figures

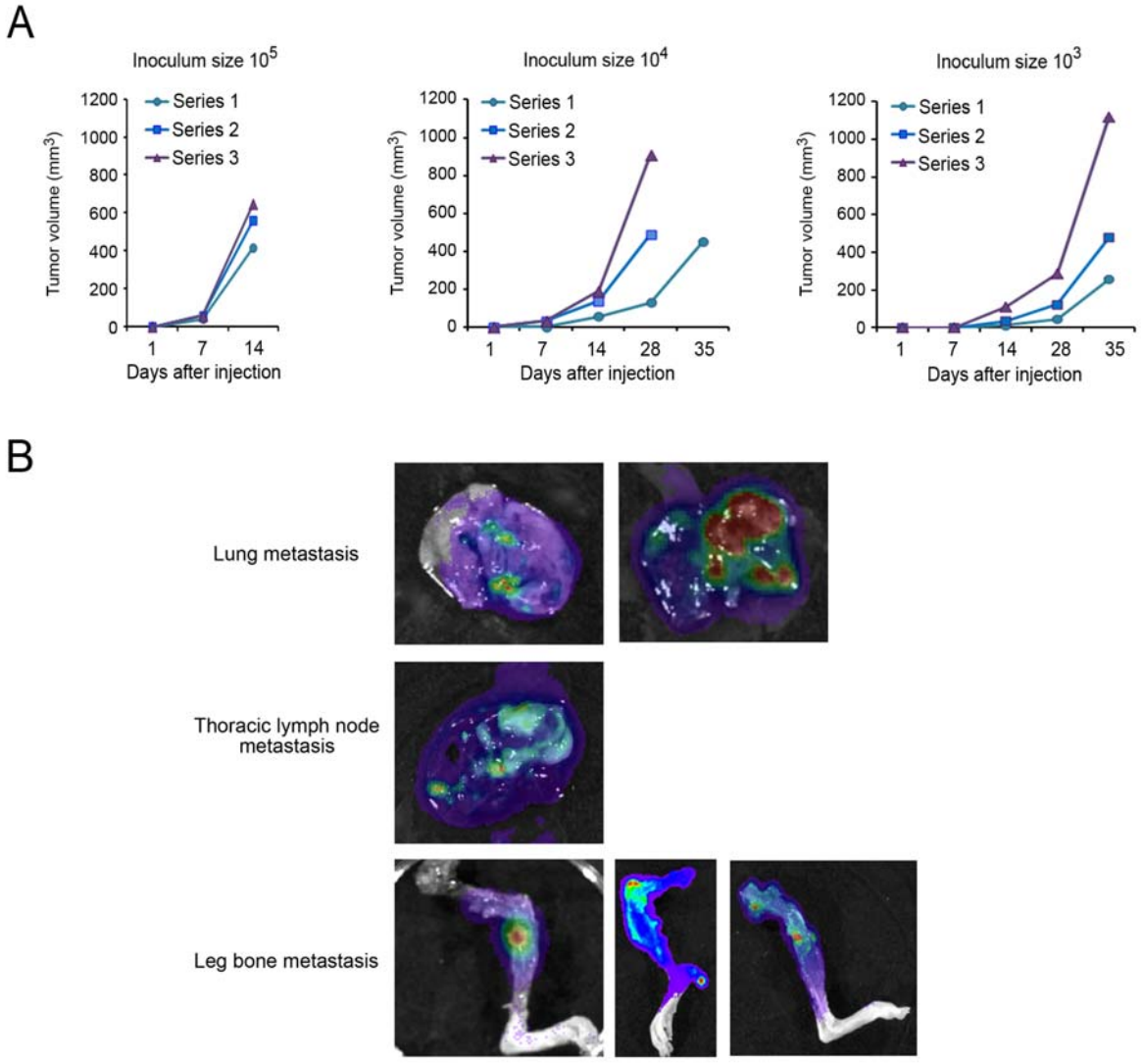

Supplemental Figure 1. Serial transplantation and metastatic growth of PC-3/Mc cells. (**A**) Serial transplantation of PC-3/Mc cells in Swiss-Nude mice. PC-3/Mc cells (10^5, 10^4 or 10^3) were implanted intramuscularly in the hind limbs of 5-week-old male Swiss-Nude mice (Series 1). Tumors formed by implantation of 10^5 cells were explanted, disgregated and reimplanted i.m. in additional mice (10^5, 10^4 or 10^3 cells) (Series 2). Newly formed tumors were equally processed and implanted in a third series of mice (Series 3). Four mice were transplanted in each series for each inoculum size. Tumors were measured with a caliper and volumes estimated as described in (1). (**B**) Bioluminescent images of metastatic tumors grown in lungs, lymph nodes and bone after intracardiac inoculation of PC-3/Mc cells. Cells (2 x 10^5) were inoculated and their growth monitored by bioluminescence (Fig. 1). At the end of the monitoring period, mice were anesthetized, administered luciferine (1.5 mg retroorbitally), sacrificed and metastatic growth detected visually with the aid of a IVIS-200 instrument. Visible metastases were removed and imaged *ex vivo*.

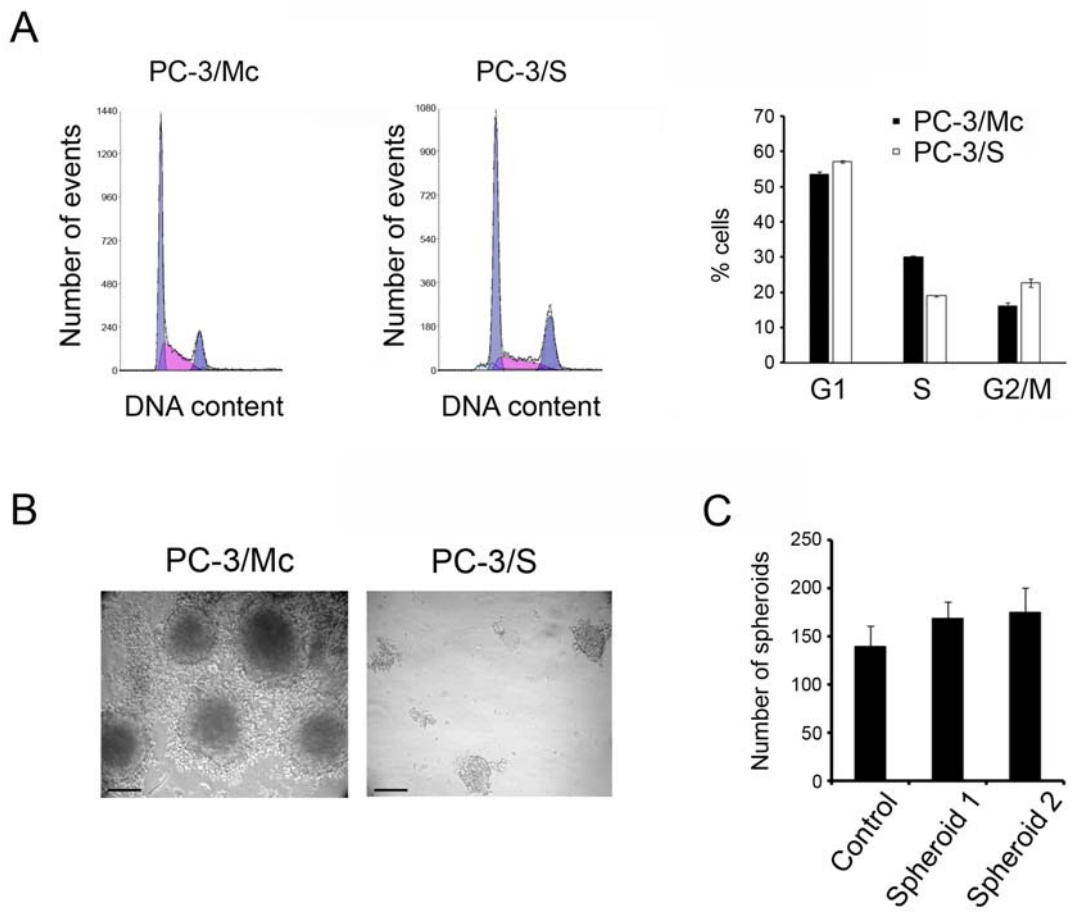

Supplemental Figure 2. Additional growth properties of PC-3/Mc and PC-3/S prostate cancer subpopulations. (**A**) Cell cycle analysis of PC-3/Mc and PC-3/S cells, with distribution histograms relative to DNA content and (right panel) distribution of populations in G1, S and M phases. (**B**) Spheroid formation assays of PC-3/Mc compared to PC-3/S cells. The figure is representative of phase-contrast images for cells grown for 14 days in low-attachment plates in medium containing 0.5% methyl cellulose Scale bar: 150 μm. (**C**) *In vitro* serial transplantation of spheroids formed by PC-3/Mc cells. Spheroids formed after 14 days of culture were dispersed, replated (10^3 cells) and grown as in (B) (Spheroid 1). The processed was repeated a third time (Spheroid 2). Graphs represent mean values and standard deviations of triplicate experiments.

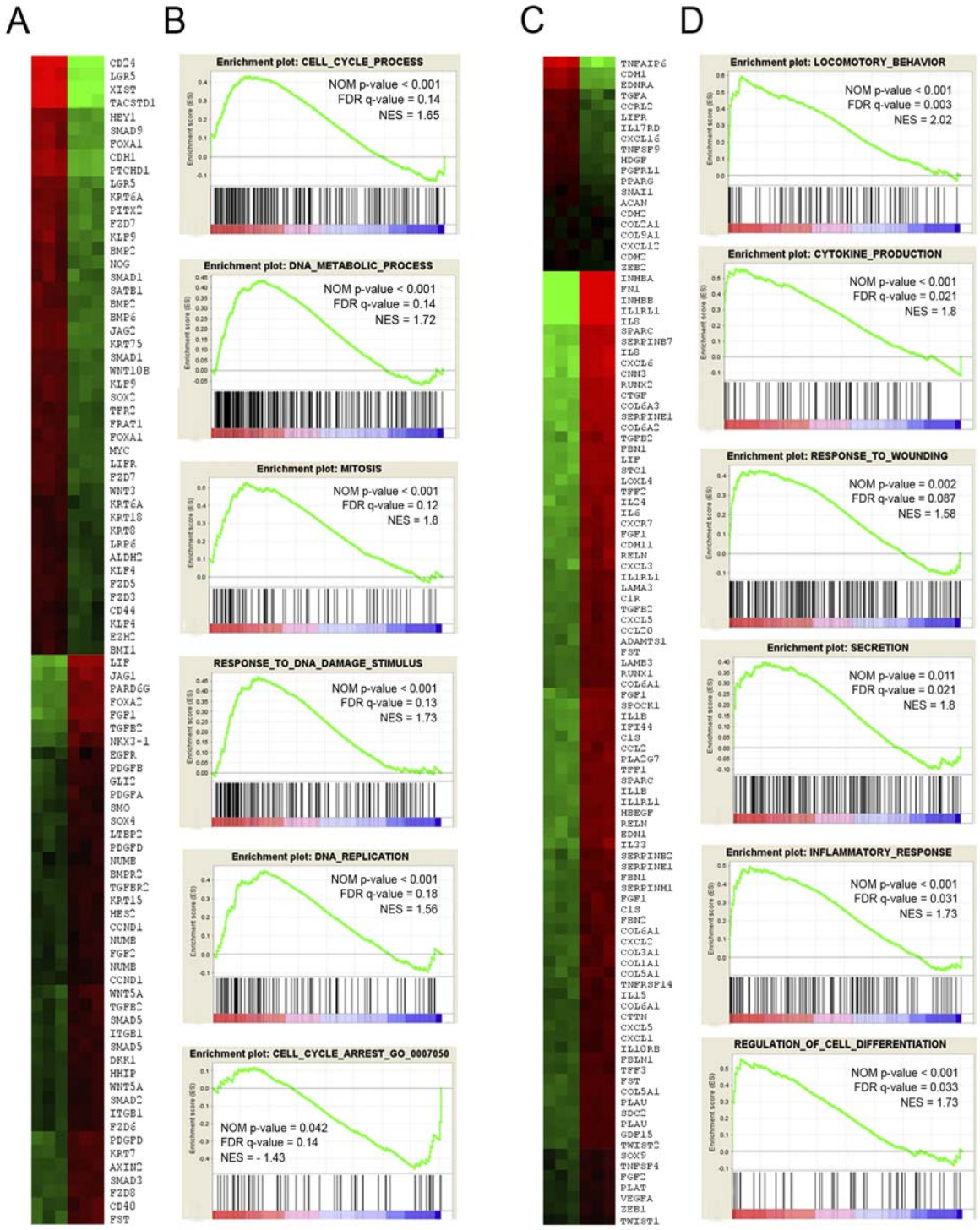

Supplemental Figure 3. PC-3/Mc cells express epithelial and self-renewal genes, while PC-3/S cells express mesenchymal genes and secretory and inflammatory gene networks. (**A**) Higher levels of expression by PC-3/Mc cells, as compared to PC-3/S cells, of epithelial genes, including E-cadherin (*CDH1*) or EpCAM (*TACSTD1*). Heatmap of normalized expression values for genes selected from a microarray analysis using Affymetrix U133A, comparing transcriptomes for PC-3/Mc and PC-3/S cells. (**B**) Enrichment in PC-3/Mc cells of gene sets for cell cycle, mitosis, DNA damage response and DNA replication. GSEA analysis was performed for microarray data comparing transcriptomes for PC-3/Mc *vs*. PC-3/S cells. (**C**) Higher levels

of expression by PC-3/S cells, relative to PC-3/Mc cells, of mesenchymal genes, including fibronectin (*FN1*), *SPARC*, *TWIST2* or *ZEB1*. Heatmap of normalized expression values for genes selected from a microarray analysis using Affymetrix U133A, comparing transcriptomes for PC-3/Mc and PC-3/S cells. (**D**) Enrichment in PC-3/S cells of gene sets for motile phenotypes, cytokines, secretion or inflammation. GSEA analysis was performed for microarray data comparing transcriptomes for PC-3/Mc *vs*. PC-3/S cells.

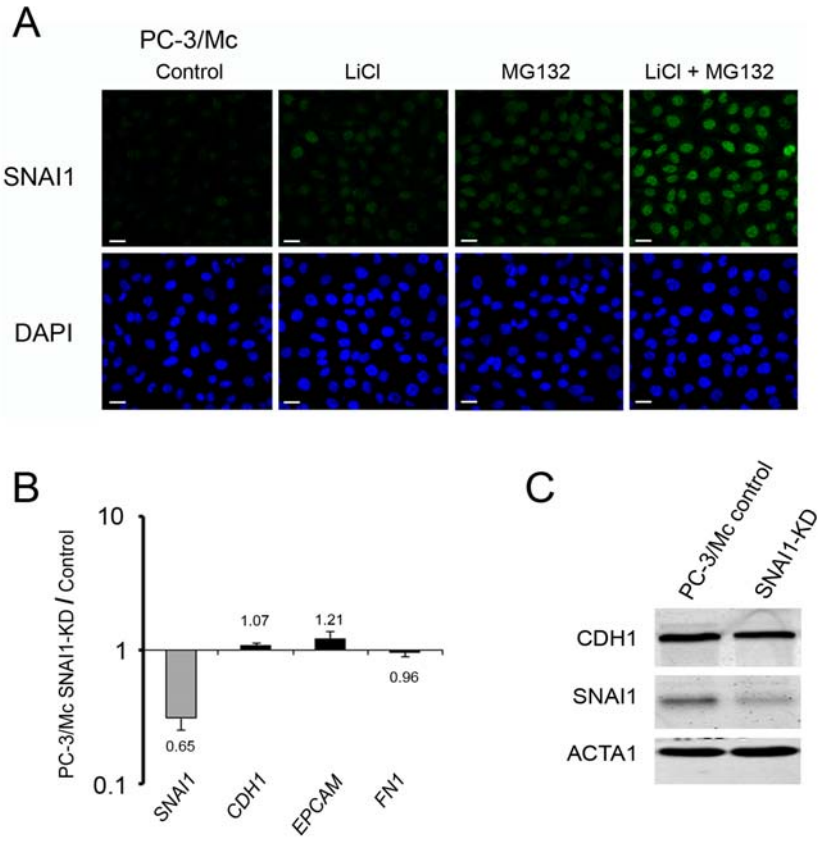

Supplemental Figure 4. Knockdown of *SNAI1* in the epithelial PC-3/Mc cells does not significantly affect the expression of E-cadherin, EpCAM or fibronectin. (**A**) Enhanced expression and nuclear localization of SNAI1 in PC-3/Mc cells by treatment for 5 hours with the GS3K inhibitor LiCl (50 mM), the proteasome inhibitor MG132 (5 μM), or both, determined by indirect immunofluorescence. Scale bar: 20 μm. (**B**) The levels of E-cadherin transcript levels in PC-3/Mc did not vary significantly after knockdown of *SNAI1*. Real-time determination of relative transcript levels of *SNAI1*, E-cadherin (*CDH1*), EpCAM (*TACSTD1*) and fibronectin (*FN1*) after knockdown of *SNAI1*. PC-3/Mc cells were lentivirally transduced with a *SNAI1*-specific shRNA, selected for puromycin resistance for over 5 days and processed for expression analyzes. Real-time Cp values were normalized to values for *RN18S1* (reference transcript), and represented as the $\log_{10}$ of ratios between knockdown and control cells. Controls were PC-3/Mc transduced with a pLK0-scrambled vector and selected for puromycin resistance. (**C**) The levels of E-cadherin protein in PC-3/Mc did not vary significantly after knockdown of *SNAI1*, as determined by Western blotting. Actin signal was used as an indicator of protein loading and transfer.

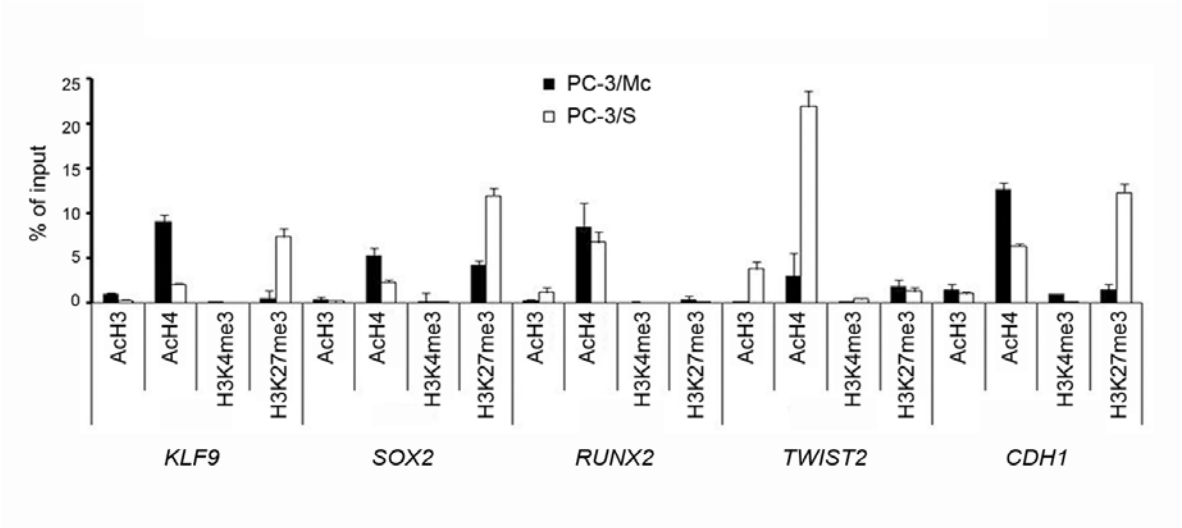

Supplemental Figure 5. Chromatin immunoprecipitation in PC-3/Mc cells showed enrichment for histone marks associated with active transcription at promoters of genes of self-renewal/pluripotency (*SOX2*, *KLF9*) and E-cadherin (*CDH1*), but not the mesenchymal genes *TWIST2* and *RUNX2*. Conversely, in PC-3/S cells, the promoters of *TWIST2* and *RUNX2* were enriched for histone marks associated with active transcription (acetyl-histone H3 and acetyl-histone H4), while the promoters of *SOX2*, *KLF9* and E-cadherin were enriched for the repressive histone mark H3K27me$_3$. The enrichment of promoter sequences after immunoprecipitation for specific histone marks was determined by real-time PCR with primers specific for each promoter, and values expressed as the percentage of the amplification values obtained for input DNA.

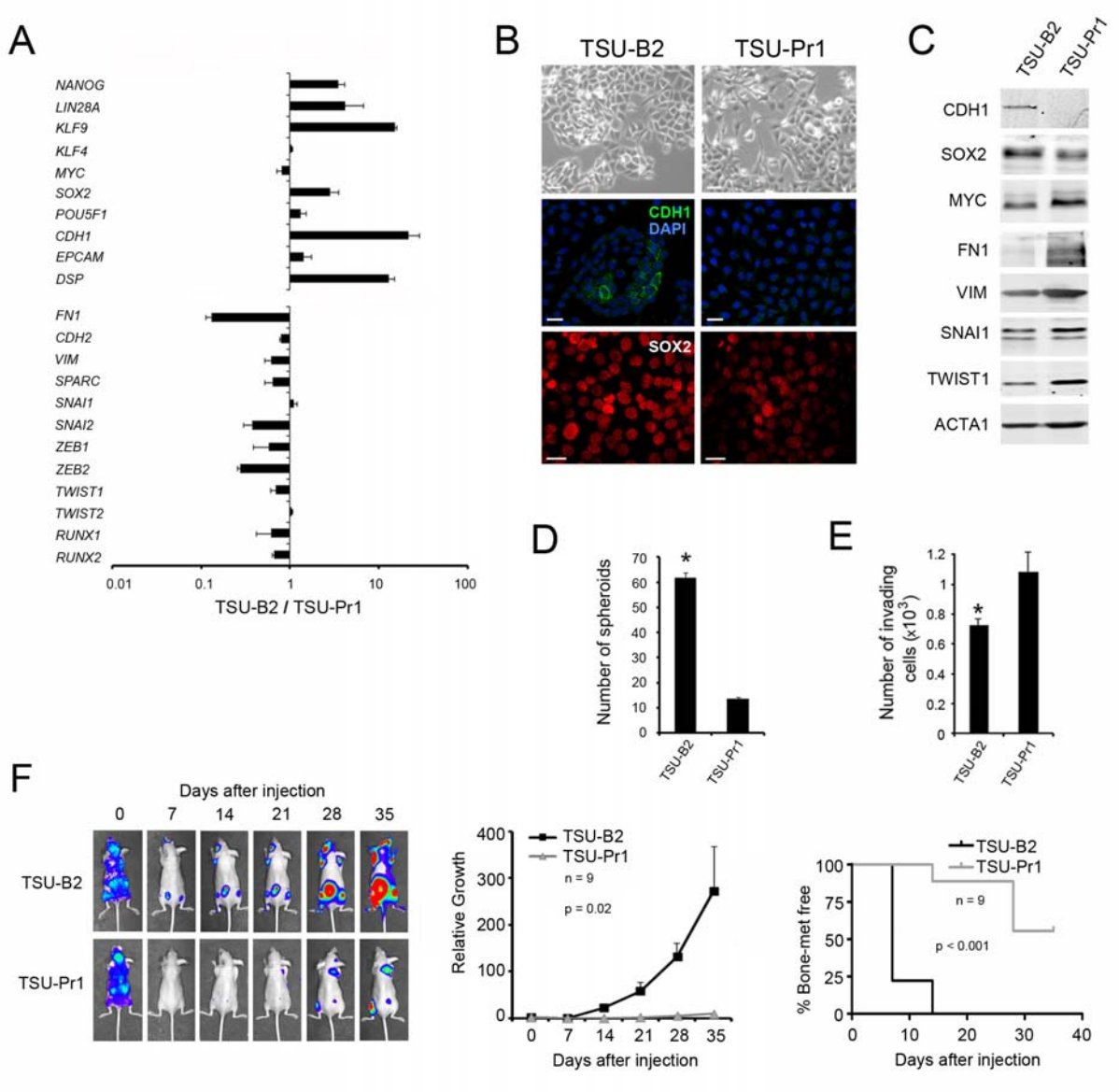

Supplemental Figure 6. Divergent phentoypes and gene programs of TSU-Pr1 *vs*. TSU-Pr1-B2 bladder cancer cell subpopulations. (**A**) TSU-Pr1-B2 cells expressed higher levels than TSU-Pr1 cells of epithelial (e.g., *CDH1*, *TACSTD1*, *DSP*) and self-renewal (e.g., *NANOG*, *LIN28*, *KLF9*, *SOX2*) genes, while TSU-Pr1 cells expressed higher levels than TSU-Pr1-B2 cells of mesenchymal genes (e.g., *FN1*, *SNAI2*, *ZEB1*, *ZEB2*, *TWIST1*). Transcripts were quantified by real-time RT-PCR and values, normalized to reference genes and expressed as the $\log_{10}$ of ratios of qPCR values between the two cell lines. (**B**) TSU-Pr1-B2 cells displayed an epithelioid morphology with a proportion of cells expressing membrane-associated E-cadherin, and TSU-Pr1 displayed a more fibroblastoid morphology, without detectable expression of E-cadherin by indirect immunofluorescence. TSU-Pr1-B2 cells also express higher levels of nuclear SOX2 than TSU-Pr-1 cells. Scale bar: 20 μm. (**C**) Comparative expression levels of epithelial, mesenchymal and self-renewal proteins in TSU-Pr1-B2 vs. TSU-Pr1 cells, determined by Western blotting. Actin signals were used as indicators of protein loading and transfer. (**D**) The more epithelial TSU-Pr1-B2 cells displayed a significantly stronger capacity to form spheroids than the more mesenchymal TSU-Pr1 cells. Cells (10^3) were seeded in low-attachment plates in medium containing 0.5% methyl cellulose. Three independent experiments were performed,

each in triplicate. Student's *t*-test: * $p < 0.05$. (**E**) The more mesenchymal TSU-Pr1 cells were significantly more invasive than the more epithelial TSU-Pr1-B2 cells in Transwell-Matrigel assays. Three independent experiments were performed, each in triplicate. Student's *t*-test: * $p < 0.05$. (**F**) Upon intracardiac injection in Ncr-nu/nu mice, the more epithelial TSU-Pr1-B2 cells grow significantly faster at different sites (middle panel) and colonize bones much more efficiently (right panel) than the more mesenchymal TSU-Pr1 cells. Mice (n = 9) were injected i.c. with 2.0×10^5 cells bearing a stably integrated firefly luciferase gene. The total tumor burden (middle panel) was estimated as the sum of photon counts for each mouse. The Kaplan-Maier plot (right panel) reflects the number of animals free of detectable bone colonization at each time point.

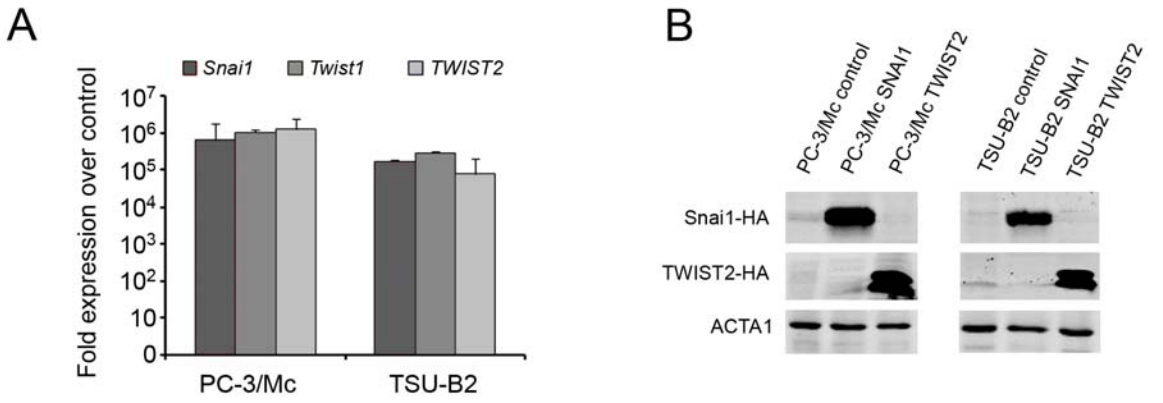

Supplemental Figure 7. Expression levels of EMT factors after retroviral transduction into PC-3/Mc and TSU-Pr1-B2 cells. (**A**) Determination by real-time RT-PCR of relative transcript levels for mouse *Snai1*, mouse *Twist1* and human *TWIST2* after retroviral transduction of the corresponding genes. Real-time Cp values were normalized to values for *RN18S1* (reference transcript) and represented as ratios between cells transduced with the experimental vectors and control cells transduced with the same empty vectors. Transcript levels for the transduced mouse *Snai1* and *Twist1* were quantified with primers and probes specific for the murine sequences. (**B**) Determination by Western blotting of protein levels of Snai1 and TWIST2 transduced into PC-3/Mc and TSU-Pr1-B2 cells, detected as proteins bearing the hemagglutinin (HA) epitope. Cells were transduced and processed as in (A). Actin signal was used as an indicator of protein loading and transfer.

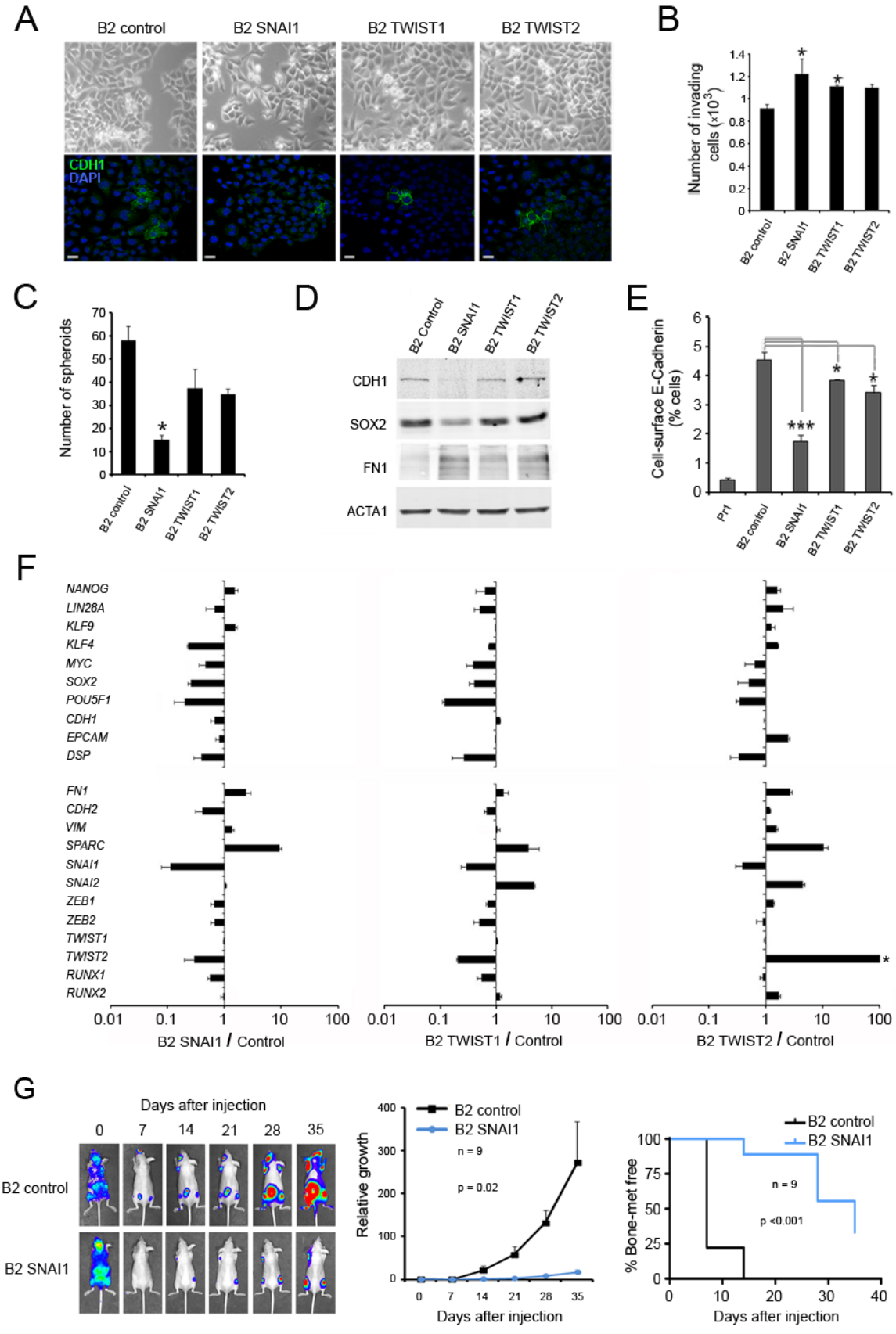
A
B2 control
B2 SNAI1
B2 TWIST1
B2 TWIST2
CDH1
DAPI
B
Number of invading cells (×10^3)
C
Number of spheroids
D
B2 Control
CDH1
SOX2
FN1
ACTA1
E
Cell-surface E-Cadherin (% cells)
Pr1
F
NANOG
LIN28A
KLF9
KLF4
MYC
SOX2
POU5F1
CDH1
EPCAM
DSP
FN1
CDH2
VIM
SPARC
SNAI1
SNAI2
ZEB1
ZEB2
TWIST1
TWIST2
RUNX1
RUNX2
B2 SNAI1 / Control
B2 TWIST1 / Control
B2 TWIST2 / Control
G
Days after injection
Relative growth
n = 9
p = 0.02
% Bone-met free
p <0.001

Supplemental Figure 8. Inhibition of TIC attributes of TSU-Pr1-B2 bladder cancer cells by constitutive overexpression of *Snai1*. (**A**) Overexpression of *Snai1* in TSU-Pr1-B2 cells induced a more fibroblastoid morphology and a decreased expression of membrane-associated E-cadherin. Controls were TSU-Pr1-B2 cells transduced with empty pBABE retroviral vector and selected for puromycin resistance. Scale bar: 20 μm. (**B**) Overexpression of *Snai1* in TSU-Pr1-B2 cells induced a significant enhancement of invasiveness in Transwell-Matrigel assays. Overexpression of *Twist1* or *TWIST2* caused a more modest effect. (**C**) Overexpression of *Snai1* in TSU-Pr1-B2 cells significantly inhibited their capacity to form spheroids in anchorage-independent growth conditions. Overexpression of *Twist1* or *TWIST2* caused a more modest effect. (**D**) Overexpression of *Snai1* in TSU-Pr1-B2 cells induced a downregulation of E-cadherin and SOX2 and an upregulation of fibronectin, as determined by Western blotting. Actin signal was used as an indicator of protein loading and transfer. (**E**) Overexpression of *Snai1* in TSU-Pr1-B2 cells caused a downregulation of cell-surface E-cadherin, as determined by flow cytometry. Overexpression of *Twist1* and *TWIST2* caused a more modest effect. (**F**) Overexpression of exogenous *Snai1* caused a downregulation of epithelial (*CDH1*, *DSP*) and of self-renewal (*KLF4*, *MYC*, *SOX2*, *POU5F1*) genes, along with an upregulation of mesenchymal genes (*FN1*, *SPARC*). The endogenous human *SNAI1* gene was strongly downregulated upon overexpression of exogenous mouse *Snai1*, as expected from its known auto-inhibitory feedback loop (18). Overexpression of *Twist1* and *TWIST2* did not significantly affect the transcript levels of E-cadherin (*CDH1*), but induced changes in the levels of transcripts for some self-renewal and mesenchymal genes. The levels of human *TWIST2* in the cells transduced with this EMT factor are off-scale. See Supplemental Figure 7 for quantification of the transduced exogenous murine *Snai1*, and murine *Twist1*. Real-time Cp values were normalized to values for *RN18S1* (reference transcript) and represented as ratios between cells transduced with the experimental vectors and control cells transduced with the same empty vector (pBABE). (**G**) Overexpression of *Snai1* strongly suppressed the growth of TSU-Pr1-B2 cells in different organs (middle panel) and their bone colonization (right panel) after intracardiac injection. Ncr-nu/nu mice (n = 9) were injected i.c. with 2.0×10^5 cells bearing a stably integrated firefly luciferase gene. The total tumor burden (middle panel) was estimated as the sum of photon counts for each mouse. The Kaplan-Maier plot (right panel) reflects the number of animals free of detectable bone colonization at each time point. For graphs with statistical analysis (Student's *t*-test): * $p < 0.05$; ** $p < 0.01$; *** $p < 0.001$.

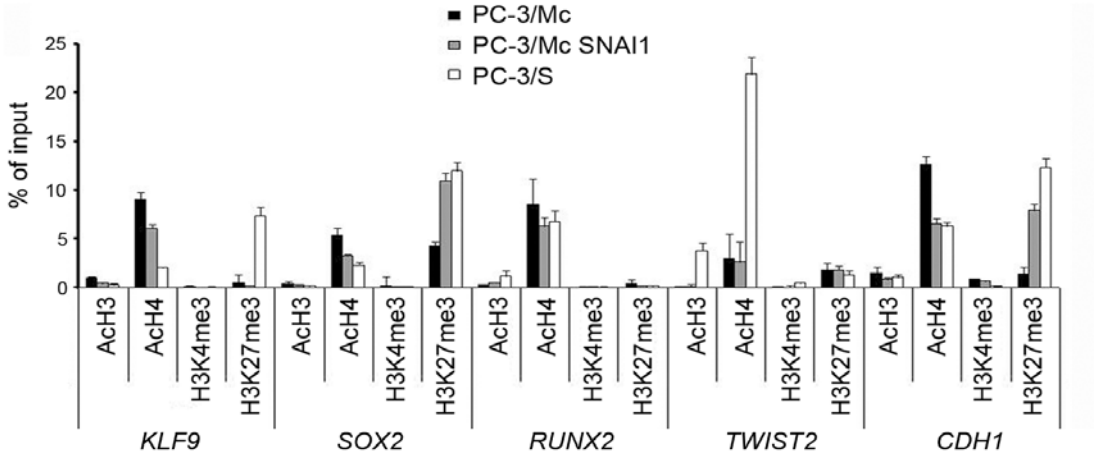

Supplemental Figure 9. Transduction and overexpression of *Snai1* in PC-3/Mc cells induced changes in histone marks associated with the promoters of *SOX2* and E-cadherin (*CDH1*), notably an enrichment of histone $H3K27_{me3}$ and depletion of acetylated histone H4, as analyzed by chromatin immunoprecipitation. For comparison, PC-3/S cells also had enriched repressive histone marks at the promoters of *SOX2* and E-cadherin.

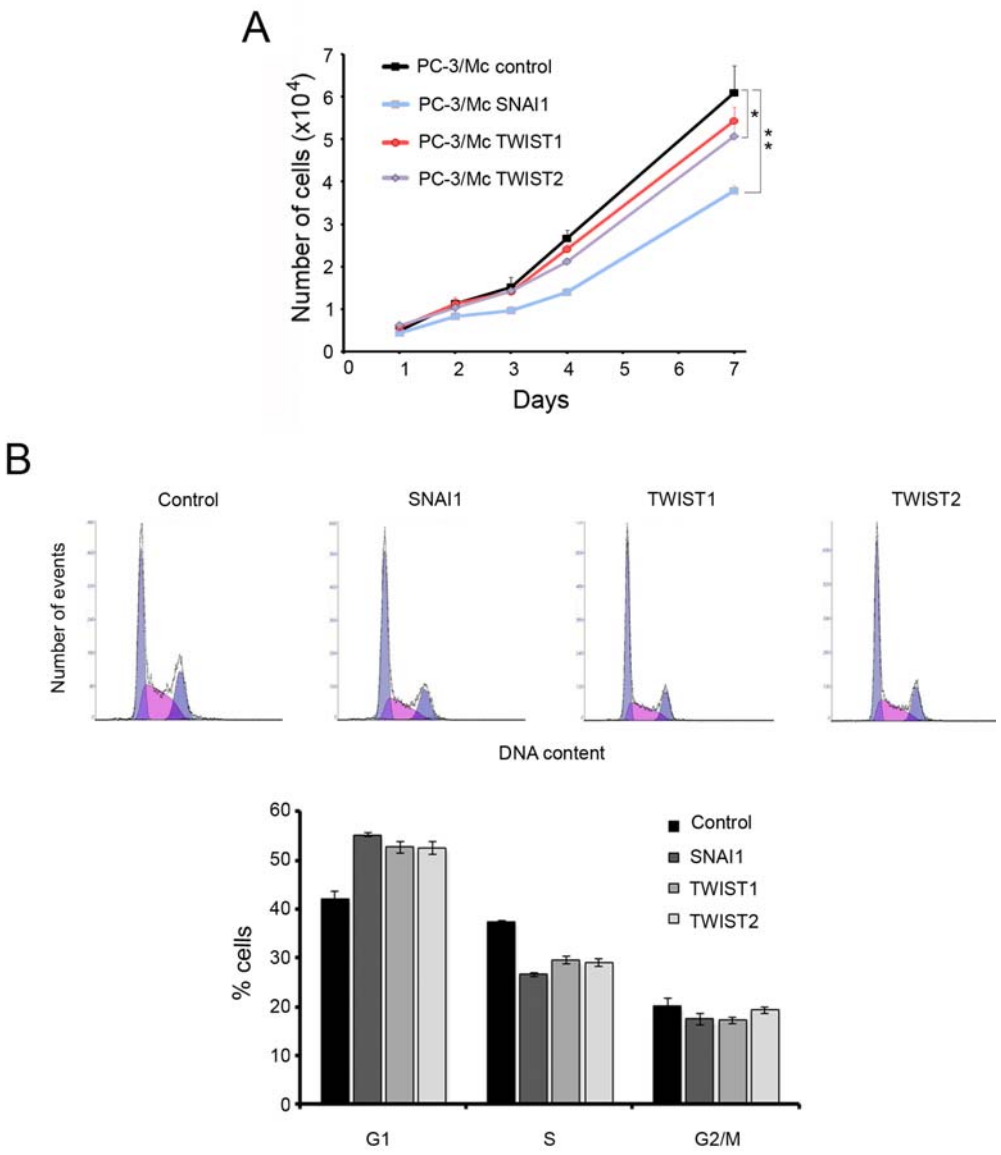

Supplemental Figure 10. Effects of the transduction and overexpression of the EMT factors *Snai1*, *Twist1* and *TWIST2* on the cell cycle profile of PC-3/Mc cells. (**A**) Overexpression of *Snai1*, *Twist1* or *TWIST2* caused a reduced growth rate on plastic, the strongest effect caused by *Snai1* overexpression. Cells (5 x 10^3) were seeded in triplicate in 96-well plates and their numbers determined 1, 2, 3, 4 and 7 days after plating. * $p < 0.05$, ** $p < 0.01$ (Student's *t*-test). (**B**) Overexpression of *Snai1*, *Twist1* or *TWIST2* caused a reduction in the proportion of cells in the S phase of the cell cycle with a concomitant increase in cells in the G phase, with the strongest effects caused by *Snai1* overexpression. Upper panels, representative DNA content histograms from flow cytometry determinations. Lower panel, histograms illustrating the quantification of cell populations in G1, S and G2-M. Experiments were done in triplicate.

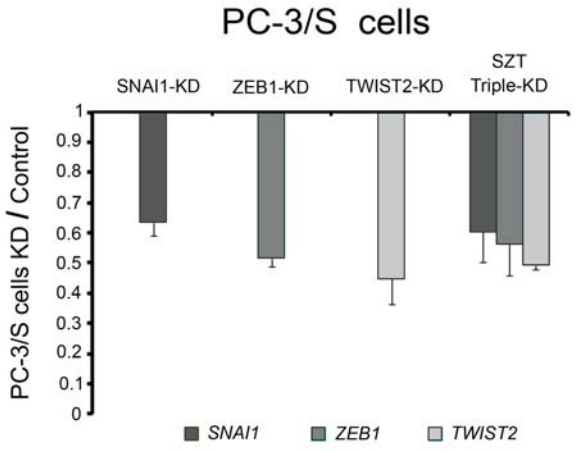

Supplemental Figure 11. Real-time RT-PCR quantification of *SNAI1*, *ZEB1* and *TWIST2* transcripts levels in PC-3/S cells knocked down for these EMT factors or a triple knockdown (*SNAI1*, *ZEB1* and *TWIST2*, SZT triple KD). Cells were transduced with lentiviral particles carrying shRNAs specific for each transcript, or for all three transcripts, selected for puromycin resistance and processed. Reference gene-normalized Cp values are represented as the ratio between experimental and control cells. Controls were PC-3/S cells transduced with a control pLK0-scrambled vector and puromycin selected. Means and standard deviations are from triplicate experiments.

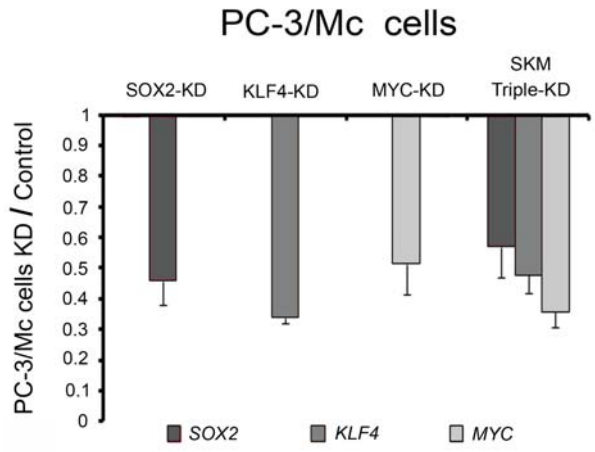

Supplemental Figure 12. Real-time RT-PCR quantification of *SOX2*, *KLF4* and *MYC* transcript levels in PC-3/Mc cells knocked down for these self-renewal/pluripotency factors or a triple knockdown (*SOX2*, *KLF4* and *MYC*, SKM triple KD). Cells were transduced with lentiviral particles carrying shRNAs specific for each transcript, or for all three transcripts, selected for puromycin resistance and processed. Reference gene-normalized Cp values are represented as the ratio between experimental and control cells. Controls were PC-3/S cells transduced with a control pLK0-scrambled vector and puromycin selected. Means and standard deviations are from triplicate experiments.

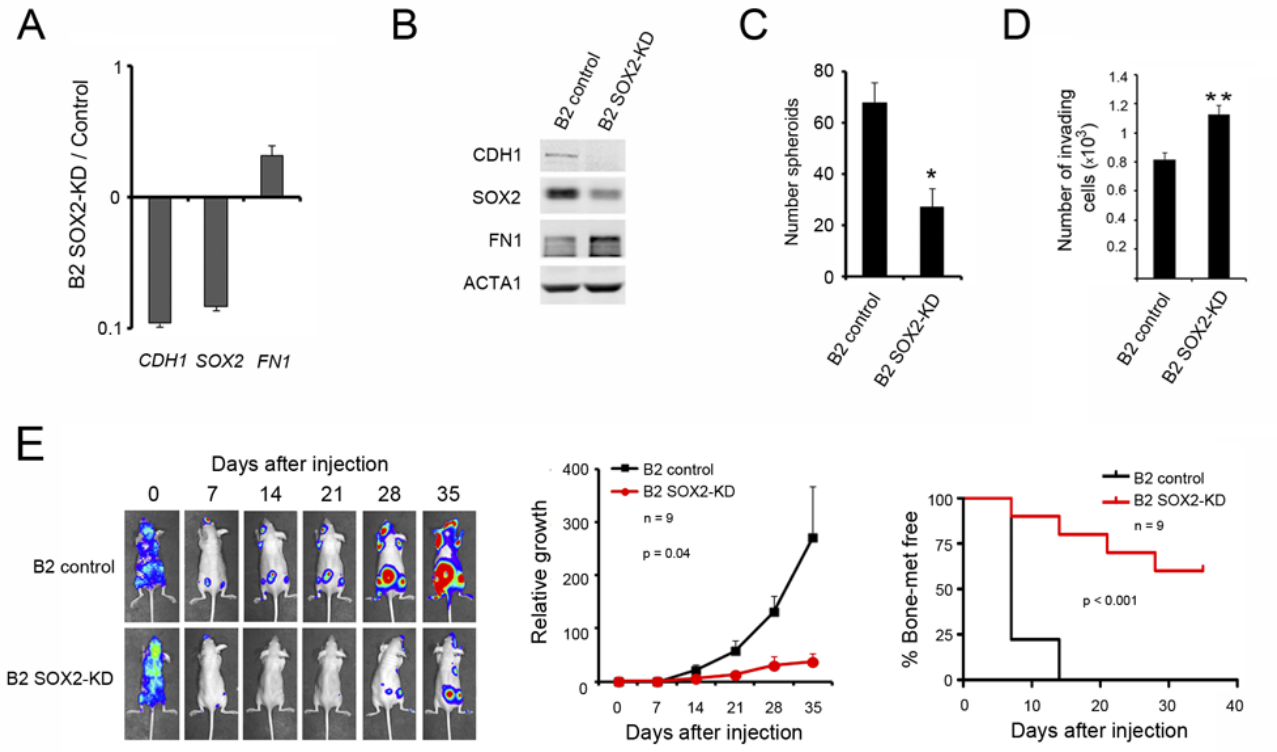

Supplemental Figure 13. Self-renewal transcription factors are required to maintain a strong epithelial program, anchorage-independent growth and metastatic potential of TSU-Pr1-B2 cells. (**A**) Knockdown of *SOX2* in TSU-Pr1-B2 cells caused a downregulation of E-cadherin (*CDH1*) and an upregulation of fibronectin (*FN1*), as determined by real-time RT-PCR. (**B**) Knockdown of *SOX2* in TSU-Pr1-B2 cells caused a downregulation of E-cadherin and an upregulation of fibronectin, as determined by Western blotting. (**C**) Knockdown of *SOX2* in TSU-Pr1-B2 cells inhibited the formation of spheroids in anchorage-independent growth conditions. Cells (10^3) were seeded in low-attachment plates in the presence of 0.5% methyl cellulose. Assays were performed in triplicate. (**D**) Knockdown of *SOX2* in TSU-Pr1-B2 cells enhanced their invasiveness in Transwell-Matrigel assays. Assays were performed in triplicate. (**E**) Knockdown of *SOX2* in TSU-Pr1-B2 cells inhibited the growth in different organs (middle panel) and bone colonization (right panel) after intracardiac injection. Ncr-nu/nu mice (n = 9) were injected i.c. with 2.5 x 10^5 cells bearing a stably integrated firefly luciferase gene. The total tumor burden (middle panel) was estimated as the sum of photon counts for each mouse. The Kaplan-Maier plot (right panel) reflects the number of animals free of detectable bone colonization at each time point. For graphs with statistical analysis (Student's *t*-test): * $p < 0.05$; ** $p < 0.01$.

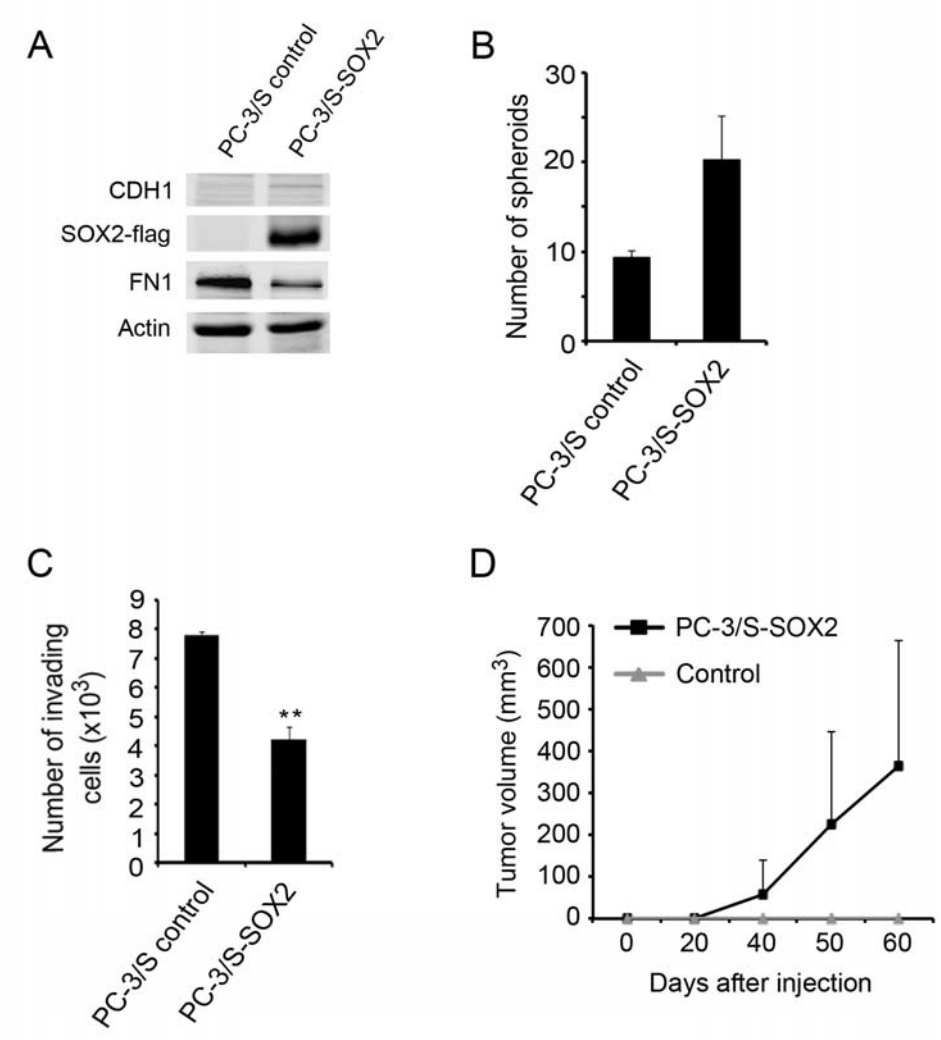

Supplemental Figure 14. Transduction and overexpression of *SOX2* in the mesenchymal-like PC-3/S cells enhances their anchorage-independent growth and tumorigenicity. (**A**) Overexpression of *SOX2* in PC-3/S cells caused an upregulation of E-cadherin and a downregulation of fibronectin, as determined by Western blotting. Controls were PC-3/S cells transduced with retroviral particles containing the empty pBABE-puro vector and selected for puromycin resistance. (**B**) Overexpression of *SOX2* in PC-3/S cells caused a gain in their capacity to form spheroids in low-attachment plates in the presence of 0.5% methyl cellulose. Assays were done in triplicate. (**C**) Overexpression of *SOX2* in PC-3/S cells inhibited their invasiveness, as determined in Tranwell-Matrigel assays. Assays were done in triplicate. Student's *t*-test: ** $p < 0.01$. (**D**) Overexpression of *SOX2* strongly enhanced the tumorigenicity of PC-3/S cells. Cells (5×10^5) were implanted i.m. in the hind limbs of male Swiss-nude mice and tumor growth monitored with a caliper (n = 4).

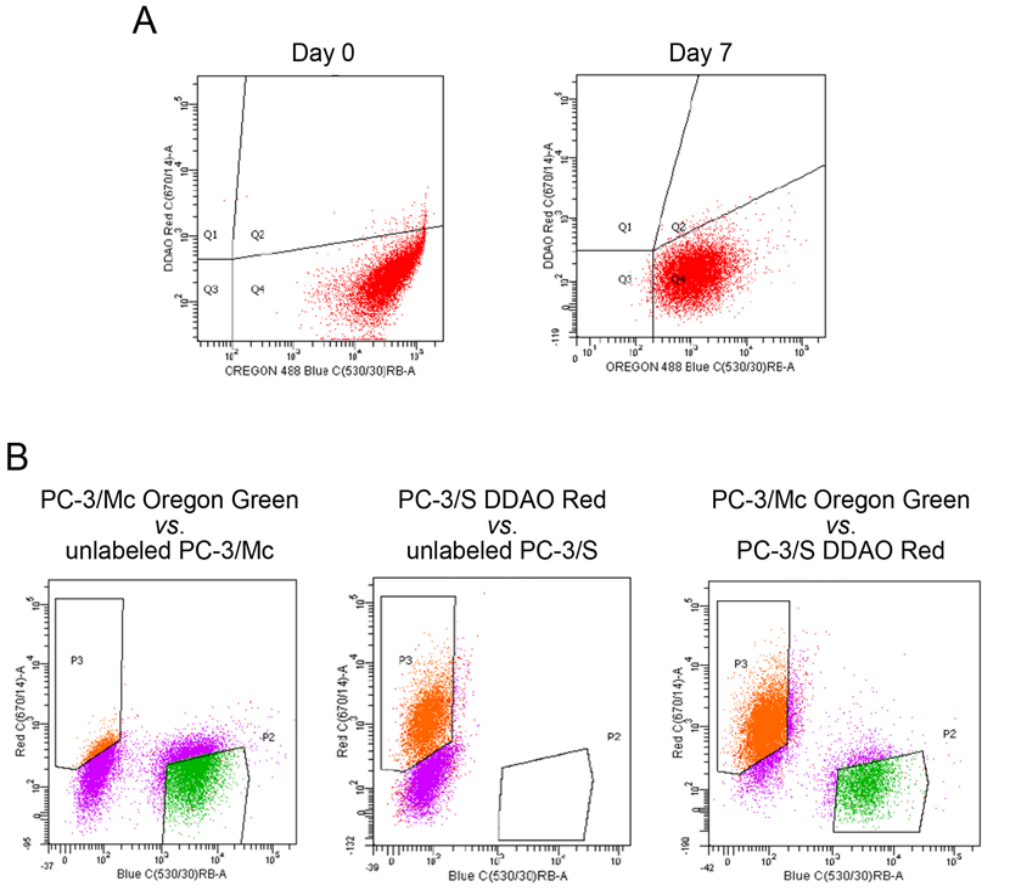

Supplemental Figure 15. Fluorophore loading and separation by FACS in cell co-culture experiments. (**A**) Loading with fluorophores is maintained for a prolonged period of time. PC-3/Mc cells were loaded with Oregon Green and examined for fluorescent levels on the same day of the loading and after 7 days in culture. (**B**) Loading, co-culture and FACS separation of PC-3/Mc cells (loaded with Oregon Green) and PC-3/S cells (loaded with DDAO Red). After loading with their respective fluorophores, PC-3/Mc and PC-3/S cells were either co-cultured or not for 48 h, and submitted to two-channel FACS (488 nm and 670 nm). The selection windows were designed so as to avoid any overlapping between green- and red-labeled cells.

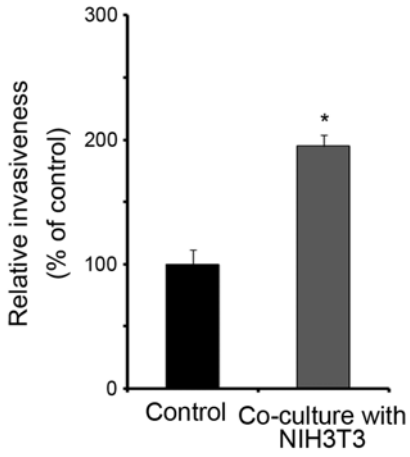

Supplemental Figure 16. Co-culture with NIH3T3 mouse fibroblasts enhanced the invasiveness of PC-3/Mc cells in Transwell-Matrigel assays. Equal numbers of PC-3/Mc cells pre-loaded with Oregon Green and NIH3T3 cells pre-loaded with DDAO Red were seeded together and assayed for invasiveness on Transwell-Matrigel assays. After 24 h, cells that had invaded into the lower chamber were quantified by flow cytometry set at 488 nm (for green fluorescent cells) and 670 nm (for red fluorescent cells). Experiments were done in triplicate. Student's *t*-test: * $p < 0.05$.

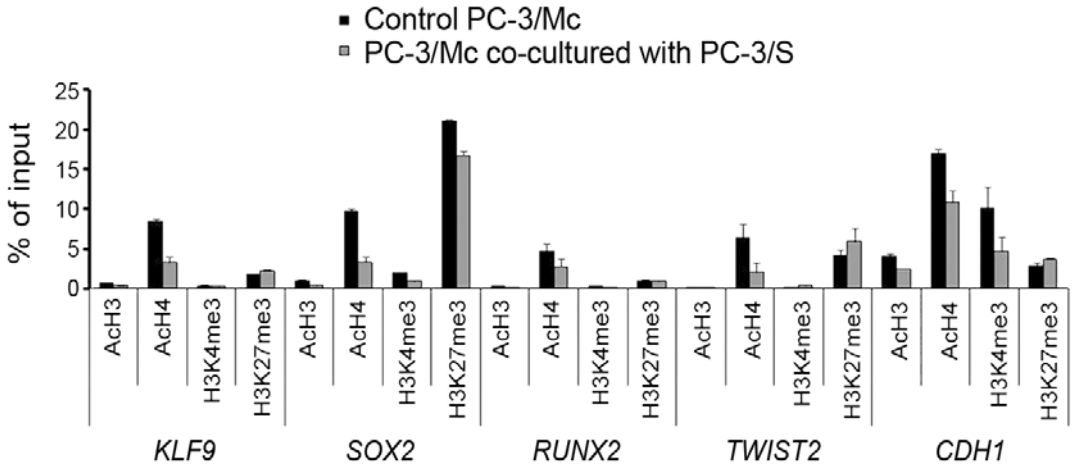

Supplemental Figure 17. Co-culture of PC-3/Mc cells with PC-3/S cells induces changes in histone marks associated with the promoters of *SOX2* and E-cadherin (*CDH1*). Most notably, the *SOX2* promoter in PC-3/Mc cells was depleted of the active transcription mark acetylated histone H4 and the *CDH1* promoter was depleted of the active transcription marks acetylated histones H3 and H4 and histone $H3K4_{me3}$. PC-3/Mc cells pre-loaded with Oregon Green and PC-3/S cells pre-loaded with DDAO Red were co-cultured for 48 h, separated by FACS and PC-3/Mc cells analyzed for histone marks by chromatin immunoprecipitation with specific antibodies, and enrichment of promoter sequences quantified by real-time PCR. Results are expressed as specific amplification levels on immunoprecipitated DNA relative to the amplification levels yielded by input DNA. All determinations were done in triplicate.

Supplementary Table 6. Expression of cell surface markers in parental PC-3 cells and derived clones PC-3/Mc and PC-3/S, determined by flow cytometry.

Surface Markers	CD24	CD44	CD40	CD71 (Tf receptor)
PC-3 (parental)	**4.0%**	**82.0%**	**24.3%**	**4.7%**
PC-3/Mc	**39.0%**	**90.0%**	**3.6%**	**64.5%**
PC-3/S	**2.4%**	**86.0%**	**44.0%**	**15.3%**

Supplemental Table 7. Enhanced bone and lymph node colonization of PC-3/Mc cells co-injected with PC-3/S cells

Metastasis Sites	Bone	Thoracic Lymph-nodes	Adrenal gland	Abdominal Lymph-nodes	No mets
PC-3/Mc	4/8	4/4*	0/4	0/4	0/4
PC-3/S	0/8	0/4	1/4	0/4	3/4
PC-3/Mc + PC-3/S	16/20	8/10	6/10	1/10	0/10

Note: PC-3/Mc colonized adrenal glands 25 days after inoculation, an organ that PC-3/Mc cells alone were not observed to colonize upon prolonged monitoring.
Asterisk: One out of 4 mice inoculated with PC-3/S cells via intracardiac injection had one adrenal gland (but no other locations) colonized with tumor cells 75 days after inoculation.

Supplemental Tables 10-12

Supplemental Table 10. TaqMan assays used for real-time RT-PCR transcript quantification.

GENE	TAQMAN PROBE
SOX2	Hs01053049_s1
RUNX2	Hs00231692_m1
TWIST2	Hs02379973_s1
RN18S1	Hs99999901_s1

Supplementary Table 11. UPL probes and primers used for real-time RT-PCR transcript quantification.

GENE	UPL PROBE		OLIGONUCLEOTIDES 5' → 3'
NANOG	#69 (cttcctcc)	FW	atgcctcacacggagactgt
		REV	agggctgtcctgaataagca
LIN28A	#23	FW	gaagcgcagatcaaaaggag
		REV	gctgatgctctggcagaagt
KLF9	#76 (tggctgtg)	FW	ctccgaaaagaggcacaagt
		REV	cgggagaacttttaaggcagt
KLF4	#82 (cagaggag)	FW	gccgctccattaccaaga
		REV	tcttcccctctttggcttg
MYC	#34 (ctgcctct)	FW	caccagcagcgactctga
		REV	gatccagactctgacctttgc
POU5F1 (OCT4)	#52 (gggaggag)	FW	gtgcctgcccttctaggaat
		REV	ggcacaaactccaggttttct
CDH1 (E-cadherin)	#35 (agaagagga)	FW	cccgggacaacgtttattac
		REV	gctggctcaagtcaaagtcc
DSP (Desmoplakin)	#49 (tggtggcc)	FW	gaatgtttggggtggatgag
		REV	ctgaggccaggtccacac
FN1	#43 (ctgcccca)	FW	gaactatgatgccgaccagaa
		REV	ggttgtgcagatttcctcgt
CDH2 (N-cadherin)	#15 (tcctgctc)	FW	tgcacagatgtggacaggat
		REV	ccacaaacatcagcacaagg
VIM	#16 (ggaggcag)	FW	aaagtgtggctgccaagaac
		REV	agcctcagagaggtcagcaa
SPARC	#77(ggtggtgg)	FW	gtgcagaggaaaccgaagag
		REV	tgtttgcagtggtggttctg
SNAI1	#11 (cttccagc)	FW	gctgcaggactctaatccaga
		REV	atctccggaggtgggatg
SNAI2	#73 (tcctcagc)	FW	acagcgaactggacacacat
		REV	gatggggctgtatgctcct
ZEB1	#3 (ctgctggg)	FW	gggaggagcagtgaaagaga
		REV	tttcttgcccttcctttctg
ZEB2	#68 (aggagcag)	FW	aagccagggacagatcagc
		REV	gccacactctgtgcatttga
TWIST1	#6 (ttcctctg)	FW	ggcatcactatggactttctctatt
		REV	ggccagtttgatcccagtatt
RUNX1	#30 (cctcagtt)	FW	ctccctgaaccactccactg
		REV	tggggatggttggatctg
RN18S1	#40 (cagcaggc)	FW	ggagagggagcctgagaaac
		REV	tcgggagtgggtaatttgc
HMBS	#26 (cagcccag)	FW	tgtggtgggaaccagctc
		REV	tgttgaggtttccccgaat

Supplementary Table 12. Primers used for real-time quantification in chromatin immunoprecipitation experiments.

GENE		OLIGONUCLEOTIDES 5' → 3'
KLF9	FW	ACCTTTGTTAAGAGAAAGTTACACCAG
	REV	AGAGTCAATTTGAGACCCTTGC
SOX2	FW	GTCTGCCTTATGGTCCGA
	REV	AACCTTCCTTGCTTCCAC
RUNX2	FW	TACAATGAGTTACAGATTCACAAGT
	REV	TCATATTTGCTGGGTGGC
TWIST2	FW	GCCAAGACCCACACAGGT
	REV	AGATGCGCTCCCAGAAGAT
CDH1	FW	CCACGCACCCCCTCTCAGT
	REV	GAGCGGGCTGGAGTCTGAAC